Review

Structure–function–folding relationships and native energy landscape of dynein light chain protein: nuclear magnetic resonance insights

P M Krishna Mohan[#] and Ramakrishna V Hosur[*]

*Department of Chemical Sciences, Tata Institute of Fundamental Research, Homi Bhabha Road,
Mumbai 400 005, India*

[#]*Present address: Department of Chemistry and Chemical Biology, Rutgers University,
610 Taylor Road, Piscataway, NJ – 08854, USA*

[*]*Corresponding author (Fax, 91 22 2280 4610; Email, hosur@tifr.res.in)*

The detailed characterization of the structure, dynamics and folding process of a protein is crucial for understanding the biological functions it performs. Modern biophysical and nuclear magnetic resonance (NMR) techniques have provided a way to obtain accurate structural and thermodynamic information on various species populated on the energy landscape of a given protein. In this context, we review here the structure–function–folding relationship of an important protein, namely, dynein light chain protein (DLC8). DLC8, the smallest subunit of the dynein motor complex, acts as a cargo adaptor. The protein exists as a dimer under physiological conditions and dissociates into a pure monomer below pH 4. Cargo binding occurs at the dimer interface. Dimer stability and relay of perturbations through the dimer interface are anticipated to be playing crucial roles in the variety of functions the protein performs. NMR investigations have provided great insights into these aspects of DLC8 in recent years.

---

1. Introduction

In a living cell, a polypeptide chain chooses between three potential fates – functional folding, potentially deadly misfolding and mysterious non-folding (Dobson 2003). This choice is dictated by the peculiarities of amino acid sequence and/or by the pressure of environmental factors. A few years back, a protein quartet model (figure 1A) was proposed for generalization of the structure–function paradigm (Uversky 2002). According to this model, biological function arises as a result of interplay between four specific conformational forms, namely, native state (ordered forms), molten globules, pre-molten globules and denatured state (random coils). In view of this, it will not be an exaggeration to assume an ensemble existence of all the four states at any particular time, their relative abundance being governed by basic

thermodynamics. Upon ligand binding or some signalling modification, the concentration of one state may increase at the expense of the others. This can explain the fast regulatory steps involved in various biological functions. Thus, the quartet model and variations thereof form the basis of the folding–function paradigm.

A complete understanding of the protein folding process requires characterization of all the species that populate along the folding coordinate. These include the unfolded state, partially folded intermediate states, low energy excited states and the fully folded native state. The most recent and widely accepted model is the 'funnel view' of protein folding (Bryngelson *et al.* 1995; Dill and Chan 1997; Onuchic *et al.* 1997; Shoemaker *et al.* 1999; Wolynes 2005) also known as the 'energy landscape model' (figure 1B), which is inclusive of the earlier concepts of 'folding pathways'. According

---

to this model, protein folding is a parallel, diffusion-like motion of conformational ensemble on the energy landscape biased towards the native state. This model is free from the Levinthal paradox (Levinthal 1969; Dill and Chan 1997) as it envisages the process of reaching a global minimum in free energy as a rapid process occurring by multiple routes on a funnel-like energy landscape (figure 1B). This view focuses on the rapid decrease of conformational heterogeneity in the course of the folding reaction and is based on a statistical description of a protein's potential surface (Wolynes *et al.* 1995; Wolynes 2005). The depth in the funnel represents the free energy of the polypeptide chain in fixed conformations and the width indicates the chain entropy (figure 1B). The funnel becomes narrower in the lower energy region because of the low chain entropy. The broad end of the funnel reflects the heterogeneous unfolded state, while the narrow end represents the supposedly homogeneous native state (Dill and Chan 1997; Dobson and Karplus 1999; Dyson and Wright 2005). Different members of the ensemble may fold/unfold along independent pathways and their energy profiles could be different. Protein folding theories start from the unfolded state (figure 1B) and encompass a range of topologies such as the pre-molten globule, the molten globule and various other ordered or disordered forms as the protein folds down the funnel (Dunker *et al.* 2002; Uversky 2002).

2.   Dynein molecular motor

Dyneins are large multicomponent microtubule-based molecular motor complexes that generate force towards the minus end of microtubules. Dyneins are broadly classified into axonemal dyneins (or flagellar dyneins) and cytoplasmic dyneins (Hook and Vallee 2006). Cytoplasmic dynein (figure 2) is a 1.2 MDa multisubunit protein complex composed of two copies each of six polypeptides (King 2000; Pfister 2005). The C-terminal regions of two identical heavy chains (~530 kDa) contain the motor domains, microtubule-binding sites, and the ATP-binding and hydrolysis sites. The heavy chains dimerize through their N-terminals, which also contain binding sites for the light intermediate chain (~50–60 kDa) and intermediate chain (~70–80 kDa) polypeptides. Cytoplasmic dynein contains three distinct families of light chains (~8–22 kDa) – Tctex1, Roadblock and dynein light chain protein (DLC8). The intermediate chains, light intermediate chains and three light chains form the cargo-binding domain of cytoplasmic dynein (King *et al.* 1996a, b; Pfister *et al.* 1996; King 2000; Harrison and King 2000; Fan *et al.* 2001). Among all these subunits, DLC8 is the smallest. Interestingly, DLC8 is known to be present in axonemal dyneins as well.

3.   Biological role of the dynein light chain protein

DLC8 is a highly conserved protein that is found in all organisms. Interestingly, the sequence is also present in rice and *C. elegans* (King and Patel-King 1995), which do not have any flagella. This indicates that the protein might be also required in non-flagellated cells. Moreover, *Drosophila* DLC8 has 94%, 71% and 50% sequence homology with DLC8 from human and rat, *Aspergillus nidulans* and yeast, respectively (King and Patel-King 1995; Liang *et al.*
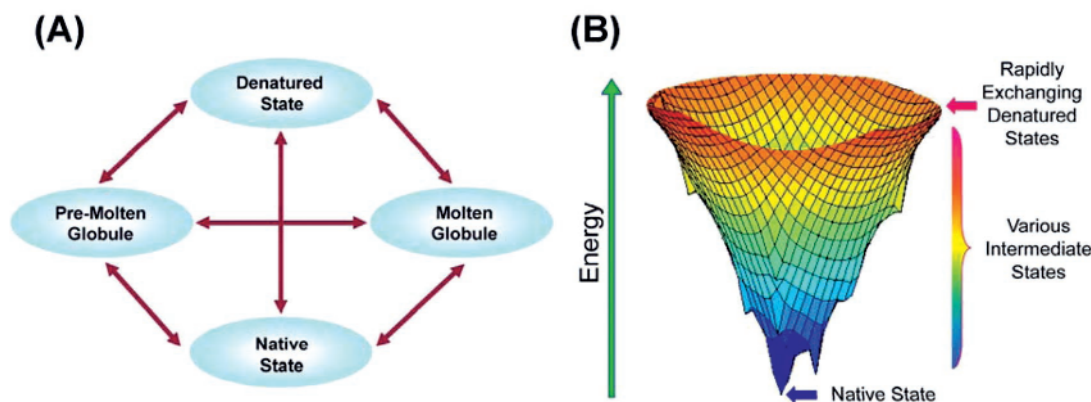

Figure 1.   **(A)** Protein Quartet Model proposed for generalization of the structure–function paradigm (Uversky 2002). The ordered state is the natively folded structure of a protein that has a well-defined secondary and tertiary structure. Molten globule states are intermediates in the protein folding pathway with compact structures that exhibit a high content of secondary structure, non-specific tertiary structure and significant structural flexibility. Pre-molten globules are condensed, but not compact and are the forms in which the unfolded chain accumulates before jumping over its folding barrier. Random coils are highly unstructured protein denatured states. **(B)** A schematic energy landscape view of protein folding. The surface of the funnel represents a whole range from the multitude of denatured conformations to the unique native structure (Dill and Chan 1997).
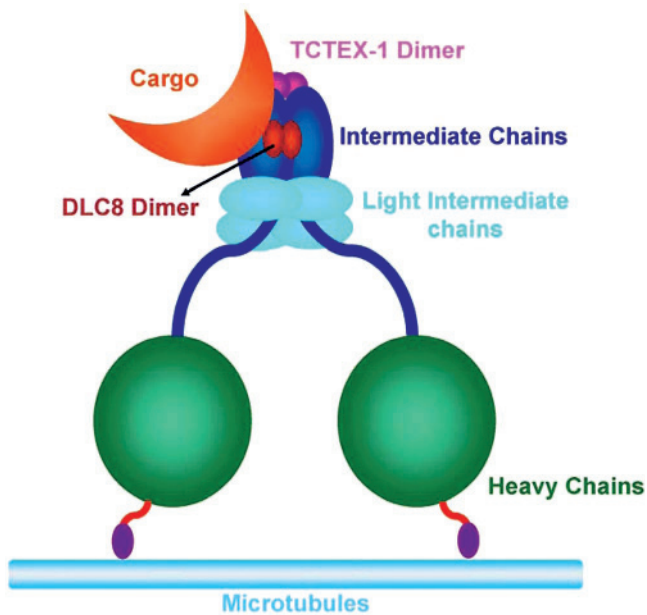
Figure 2. Schematic showing the assembly of the dynein motor complex

1999). King *et al.* (1996a) observed that multiple forms of the protein are present in the mammalian system and it is not always associated with the dynein–dynactin complex. Subsequently, the DLC8 gene was cloned from *Drosophila* and human and it was found to be ubiquitously expressed in *Drosophila* (Dick *et al.* 1996). Cross-linking studies revealed that DLC8 is mainly a dimer in solution and is a part of not only cytoplasmic dynein, but also of MyosinV (Benashski *et al.* 1997). The high sequence similarity and evolutionary conservation indicates that the protein must have multi-regulatory functions.

DLC8 associates with dynein by virtue of a physical interaction with the dynein intermediate chain (IC74) subunit, and a 10 amino acid stretch between residue 147 and 157 at the N-terminus of IC74 is essential and sufficient to bind DLC8 (Lo *et al.* 2001). Interestingly, the same protein was independently isolated as a specific interactor of the neuronal nitric oxide synthase (nNOS) (Jaffrey and Snyder 1996), IκBα (Crepieux *et al.* 1997), guanylate kinase-associated protein (GKAP) (Naisbitt *et al.* 2000), the Nrf-1 (Ew) (Herzig *et al.* 2000) and many others outside the dynein complex (Harrison and King 2000; Vallee *et al.* 2004; Barbar 2008) by using the yeast two-hybrid system. Careful mapping analysis revealed that DLC8-binding sites in many of these interactors share a consensus motif, K/RXTQT, which was also found in IC74 (Lo *et al.* 2001). However, no such sequence motif was found in some of the bonafide partners of DLC8, for example, nNOS, GKAP, MyosinV, etc. A binding study with synthetic dodecapeptides spanning

different regions of cytoskeleton-related proteins again identified not only the same consensus motif, K/RXTQT, but also another one, GIQVD, which is present in nNOS, GKAP and many other partners (Rodriguez-Crespo *et al.* 2001). Further, proteomic analyses have uncovered many interesting candidates, for example, Dynamin2, Dynamin3, Myosin-X, etc. (Navarro-Lerida *et al.* 2004). Recently, studies on p21-activated kinase 1 (Pak1), a member of the evolutionarily conserved family of serine/threonine kinases, revealed DLC8 as its physiological interacting substrate with binding sites mapped to amino acids 61–89 and the phosphorylation site at Ser 88 (Vadlamudi *et al.* 2004). The phosphorylation of DLC8 by Pak1 plays a regulatory role in tumorigenesis and macropinocytosis (Vadlamudi *et al.* 2004; Yang *et al.* 2005; Song *et al.* 2008). Pak1 phosphorylation of DLC8 on Ser 88 controls vesicle formation and trafficking functions, whereas mutation of Ser 88 to Ala (S88A) prevents macropinocytosis (Yang *et al.* 2005). Moreover, DLC8 phosphorylation by Pak1 prevents interaction with the apoptotic protein Bim and plays an essential role in cell survival (Vadlamudi *et al.* 2004).

Altogether, the conserved nature, ubiquitous expression, multiple biochemical forms and numerous cellular targets of DLC8 strongly suggest that the protein might be playing a conserved cellular function in multiple protein complexes. A large body of evidence is available, mainly from biochemical interaction studies, which suggest an involvement of the conserved protein in many biological processes such as in viral transport, RNA transport, apoptosis, cancer cell cycle, inhibition of nNOS, facilitation of Swallow folding, nuclear transport, etc. (Jaffrey and Snyder 1996; Benashski *et al.* 1997; Crepieux *et al.* 1997; Sodeik *et al.* 1997; Puthalakath *et al.* 1999; Suomalainen *et al.* 1999; Leopold *et al.* 2000; Naisbitt *et al.* 2000; Schnorrer *et al.* 2000; Puthalakath *et al.* 2001; Vadlamudi *et al.* 2004). Moreover, it has been observed that, in several cases, DLC8 interacts with partially disordered proteins and promotes dimerization. Considering all these dynein-dependent and -independent functions, DLC8 has been termed as an interactive protein hub (Barbar 2008).

4. Structural characteristics of dimeric, monomeric and target-bound DLC8 dimer

The major fraction of DLC8 is a dimer (figure 3A) under physiological conditions (Benashski *et al.* 1997; Barbar *et al.* 2001) and it undergoes transition to a monomer when there is a decrease in the pH (Tochio *et al.* 1998; Barbar *et al.* 2001); the protein is a stable monomer below pH 3.5. The structure of the free monomer (figure 3B) is identical to that of the monomer in the dimer except for small differences. The dimer contains two α-helices and five β-strands (Liang *et al.* 1999; Fan *et al.* 2001), whereas the monomer contains two α-helices and four β-strands. The α and β secondary

structural elements in the dimer are α1: 15–31, α2: 35–50, β1: 6–11, β2: 54–59, β3: 62–67, β4: 72–78, and β5: 81–87. The corresponding secondary elements in the monomer are α1: 15–29, α2: 35–48, β1: 8–11, β2: 55–58, β4: 72–78, and β5: 81–87. Thus, the differences between the two structures are (i) the β3-strand in the dimer loses its secondary structure on dissociation to the monomer, and (ii) the helices α1 and α2 and the strands β1 and β2 get shortened by two residues (Makokha *et al.* 2004). The structural architecture of the DLC8 dimer suggests that both the helices in each of the monomers form the periphery of the molecule whereas the β-strands form the hydrophobic core. Among the β-strands, β1 remains unpaired, whereas β2, β3 form antiparallel β-sheets across the dimer interface in a domain-swapped manner, i.e. β2 forms an antiparallel β-sheet with β3' (i.e. β3 of another monomer) and vice versa; further, in each monomer, β4 and β5 form the antiparallel β-sheets which are present in the interior of the individual monomeric units (Liang *et al.* 1999). A number of contacts at the interface between the two monomers stabilize the dimeric structure. These include side chain H-bonds: Gln 61–Arg 60', Tyr 65–Lys 44', Thr 67–Lys 43' and hydrophobic interactions: Ile 57/57', Phe 62/62', Ser 64/64', Val 66/66' and His 55/55' (Liang *et al.* 1999).

The structure of the DLC8–nNOS complex suggests that nNOS peptide binds to a hydrophobic groove inside the core of the dimer forming an antiparallel β-strand with the β3-strand (figure 3C and D). In the crystal structure of the DLC8–peptide complex (Liang *et al.* 1999), the peptide sits in the deep groove of the dimer, where the β3 strand forms the bottom, β4 and β5 strands form one side and the α2' helix forms the other side of the groove (figure 3C and D). Aromatic (Phe 62, Tyr 65, Phe 73, Tyr 75, Tyr 77 and Phe 86) and aliphaptic residues (Ser 64, Val 66, Ala 82, and Leu 84) line this groove. Although the groove is predominantly hydrophobic, the side chains of polar residues (Asp 12, Arg 60, Asn 61, Thr 67, His 68, Ile 34' Glu 35' and Lys 36') participate in important interactions with the bound peptide. For example, the side chain of Gln 234 of nNOS is bound in a pocket formed by residues Leu 34', Glu 35' and Lys 36' from α2', and makes hydrogen bonds to Glu 35' and Lys 36'. The bound peptide residues form antiparallel β-strand hydrogen bonds with Phe 62, Ser 64, Val 66 and His 68 of the DLC8 protein. Residues Lys 5, Val 7, Asn 10, and Asp 12 all have atoms within 4 Å from one or more atoms of the bound peptide. Several of these interactions are also seen in the structure of DLC8–Bim complex (Fan *et al.* 2001). Moreover, in this case specifically, the carboxyl group of
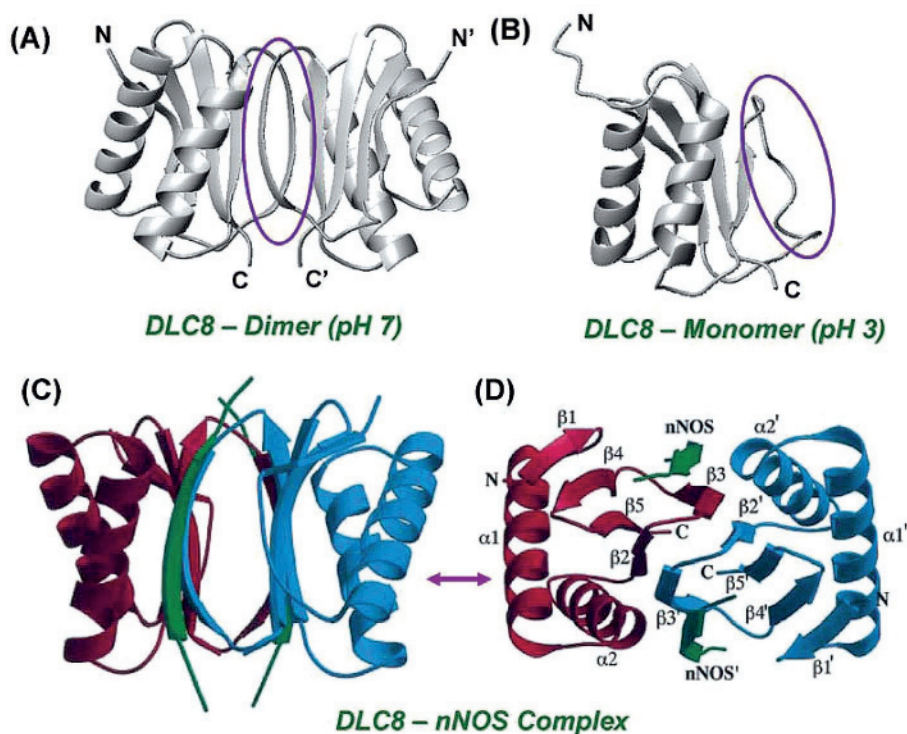

Figure 3. Structures of the dynein light chain protein dimer (pdb ID: 1f96) **(A).** dynein light chain protein monomer (pdb ID: 1rhw) **(B)** and dynein light chain protein–nNOS complex (pdb ID: 1cmi, (Liang *et al.* 1999)) **(C)** and **(D)**. **(C)** and **(D)** represent two orientations of the complex. The violet ellipse in **(A)** and **(B)** represents the β-sheet (β3 and β3') in the dimer which remains as a loop in monomer. The images were produced using Mol Mol (Koradi *et al.* 1996).

Asp 12 interacts with the positively charged $-\varepsilon NH^+_3$ group of Lys in the (K/R)XTQT sequence (Fan *et al.* 2001). Since the dimer has a two-fold symmetry, it provides two such symmetrical binding sites for the interacting peptides (Liang *et al.* 1999). Further, the numerous structural studies on the dimer–target complexes have revealed that different targets use different regions of the flexible-binding channel within the dimer and this is similar to the way calmodulin recognizes numerous cellular targets (Fan *et al.* 2001). The monomer does not bind to the target peptide (Wang *et al.* 2003) because of the absence of the β3-strand (Makokha *et al.* 2004; Wang *et al.* 2003).

5. Mechanism of pH-induced dimer dissociation

As stated above, the protein is a pure dimer under physiological conditions and a dimer-to-monomer transition can occur due to pH change. Sedimentation and NMR experiments by Barbar *et al.* (Barbar *et al.* 2001; Nyarko *et al.* 2005) suggest that the midpoint of dimer-to-monomer transition is ~pH 4.8 with a dissociation constant of 12 μM. A detailed study of this transition will throw light on the stability perturbations of the protein with regard to environmental perturbations, and hence on its function.

NMR investigations using ^{15}N transverse relaxation rates (R_2) and line broadening effects provided residue-level mechanistic insights into the dimer–monomer equilibrium (Mohan *et al.* 2006). Figure 4 shows residue-wise ^{15}N transverse relaxation rates (R_2) measured at 27 °C in DLC8 at five pH values, 7, 6, 5, 3.5 and 3. A notable feature at pH 7.0 is the appearance of very large R_2 values for the residues: (Thr 67, Arg 71, His 72, Ile 74), belonging to the loop between β3 and β4, and partly to β3 and β4. These large R_2 values are suggestive of high conformational transitions in this segment of the molecule. In fact, Fan *et al.* (2002) measured high R_{ex} values (2–10 s^{-1}) for the region aa 55–75 in the dimer at pH 7. Examination of the amino acid sequence reveals that there are three histidines (His 55, His 68, His 72) in this region. Among these, His 68, His 72 are exposed to the solvent whereas His 55 is completely buried in the hydrophobic core of the dimer. Recent NMR measurements by Barbar and coworkers (Nyarko *et al.* 2005) have found the values to be 4.5 for His 55, and 6.0 for His 68 and His 72. Thus, there will be some population (~10%) of charged His side chains even at pH 7 for His 68 and His 72. Under these conditions, there will be interconversion between protein molecules having charged and neutral His at the 68 and 72 locations, and this would account for the high R_2 values seen in that loop area at pH 7.

As the pH is reduced to 6, the population of charged His 68 and His 72 rises to 50% (for His 55, the population of charged species will be ~3%), resulting in greater conformational dynamics in the loop. As a consequence,

several neighbouring residues also acquire higher conformational flexibilities (micro- to millisecond time scale), manifesting in a scatter in the R_2s (figure 4), and causing a slow loosening of the structure in that vicinity. The signals due to the several residues become much weaker in the hetero nuclear single quantum coherence (HSQC)
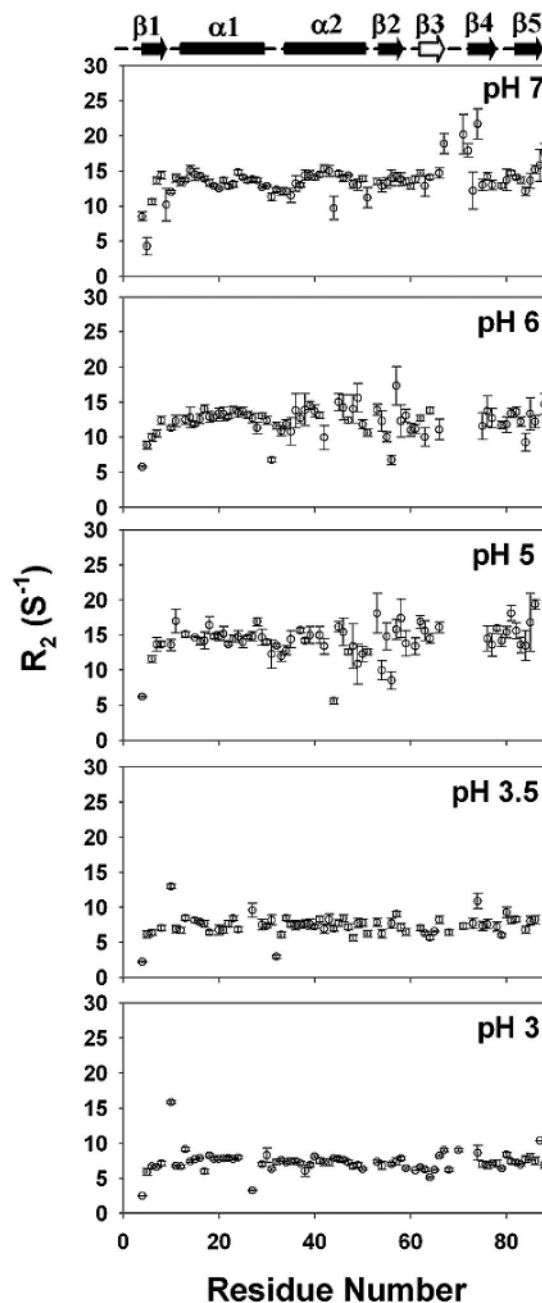

Figure 4. ^{15}N transverse relaxation rates (R_2) in DLC8 measured at various pH values, 27°C. The secondary structural elements in the protein are marked above with cylinders (for helices) and arrows (for strands). β3 which is present in the dimer only is marked with an open arrow.

spectra. This is a consequence of line broadening due to slow time-scale motions due to conformational transitions. Clearly, this indicates an extension of the conformational dynamics outwards from the loop between $\beta 3$, $\beta 4$ to other regions ($\beta 3$, $\beta 4$, $\beta 5$, beginning of the $\alpha 2$ helix, and end of $\beta 2$) of the protein. Some residues at the N-terminal and C-terminal also acquire enhanced conformational dynamics.

On further reduction of the pH to 5.0, the population of charged histidines increases further: ~90% for His 68 and His 72, and ~25% for His 55. The residues in the C-terminal β-sheet start to show a scatter in the R_2 values indicating further extension of conformational dynamics (figure 4). Besides, some more peaks vanish due to slow time-scale conformational transitions. Further, the conformational fluctuations seen at the residues of the dimer interface, Arg 60, Tyr 65, Thr 67 and Lys 43, would contribute to destabilization of the H-bonds: Gln 61–Arg 60', Tyr 65–Lys 44', Thr 67–Lys 43' between the two monomer units across the dimer interface. Similarly, this conformational dynamics would also lead to a partial loss of the hydrophobic interactions, Val 66/66' and His 55/55'. Thus, the observed protein dynamics clearly indicates a hierarchy of conformational transitions with pH change and indicates progressive loosening of the dimeric structure. Explicitly,

loosening of the dimeric structure gets initiated at the dimer interface in the loop between $\beta 3$, $\beta 4$ and end of $\beta 5$ and then travels through $\beta 3$, $\beta 4$, $\beta 5$, helix $\alpha 2$ and end of $\beta 2$ (figure 4).

Once the pH is reduced further below 3.5, His 55 protonation increases to nearly 90–100%, causing enhanced repulsion. Moreover, accommodation of charged His 55 in the hydrophobic pocket will also be highly unfavourable in the dimer. It has been established on the basis of mutational and pH titration studies that at low pH, His 55 gets protonated in the side chain, and since the two histidines (His 55/55') from the two monomers are only 5.7 Å apart, this results in charge–charge repulsion causing dissociation of the dimer into the monomers (Barbar and Hare 2004; Barbar *et al.* 2001). As a consequence, the dimer becomes energetically unstable and dissociates into monomers. The formation of a stable monomer structure is evident from the transverse relaxation data in figure 4 as the average R_2 values have reduced to nearly half of those in the dimer (pH 5–7).

In the light of all these observations, a step-by-step mechanism for pH-induced dimmer-to-monomer transition was proposed (Mohan *et al.* 2006) and is depicted in figure 5. Progressive increase in conformational transitions with decreasing pH is shown by a green colour in the different segments of the protein structure. At physiological pH, the
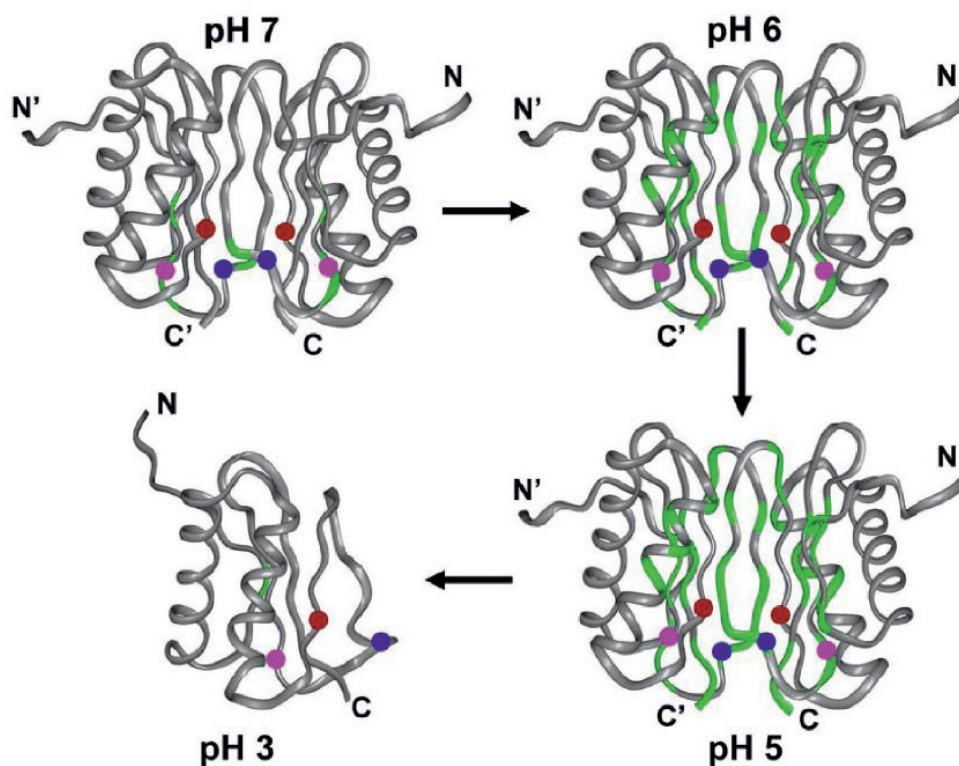

Figure 5. Schematic diagram showing the mechanism of transition of DLC8 from dimer to monomer induced by pH change. The segments marked with green identify the regions of conformational exchange. The locations of the histidines (three in each monomer) are indicated by coloured balls: His 55/55' is brown, His 68/68' is blue and His 72/72' is pink.

loop between *β*3 and *β*4 has high conformational flexibility in the milli- to microsecond time scale (large R_2 values), which can be attributed to partial protonation of His 68 and His 72 (the positions of the three histidines in each monomer are indicated by coloured balls in the figure 5). At pH 6, this flexibility increases and a few more residues belonging to *β*3, *β*4, *β*5, beginning of the *α*2 helix and end of *β*2 acquire flexibility. An increase in the population of protonated His at positions 68 and 72 would cause strand repulsions between *β*3–*β*3', *β*4–*β*4' and *β*3/*β*3'–*β*4/*β*4'. At pH 5.0, even larger segments belonging to *β*4/*β*4', *β*5/*β*5', *β*2/*β*2' and *α*2/*α*2' acquire enhanced conformational flexibility. A larger population of charged His 55 (which belongs to the *β*2-strand) results in enhanced repulsion between the strands: *β*2–*β*3', *β*2'–*β*3, *β*2–*β*2' and *β*2/*β*2'–*β*4/*β*4'. All these result in loosening of the other H-bond interactions and hydrophobic interactions at the dimer interface. Finally, at pH 3.0, the population of protonated histidines increases further, so much so that dimer formation is no longer energetically favourable and the dimer dissociates into monomers.

6. Stability of the native state: dissection at residue level

Equilibrium unfolding experiments provide a wealth of information related to protein stability and the nature of the species present along the unfolding coordinate. Circular dichroism (CD) and steady-state fluorescence have been the two most useful probes to study the global features of the equilibrium unfolding pathways, and NMR spectroscopy furnishes residue-level details for all the species present along the folding coordinate. The stability and unfolding features of the DLC8 protein, both in its dimeric and monomeric forms, have been studied extensively with various denaturants such as urea, temperature, guanidine hydrochloride (GdnHCl), pH, etc. (Barbar *et al.* 2001; Chatterjee *et al.* 2007; Krishna Mohan 2007; Krishna Mohan *et al.* 2008; Mohan and Hosur 2008a; Krishna Mohan *et al.* 2009; Mohan *et al.* 2009a, b) using various biophysical techniques. Complete thermal unfolding studies on the DLC8 dimer are not feasible as the dimer forms soluble and insoluble aggregates above 65ºC (Barbar *et al.* 2001; Krishna Mohan 2008). Detailed investigations on the unfolding behaviour of the DLC8 dimer using GdnHCl have provided valuable insights on the differential stability characteristics of the dimer and also on the nature of intermediates present in the unfolding transition. The denaturation curves of the DLC8 dimer at pH 7 with GdnHCl obtained by means of far-UV CD spectroscopy and by fluorescence spectroscopy by monitoring the fluorescence property of the single tryptophan residue (W54) are shown in figure 6A. The former reflects secondary structural changes, and the latter reflects tertiary structural changes. It is evident from figure 6A that the denaturation curves obtained from CD and fluorescence do not superimpose, suggesting that the equilibrium unfolding of the protein is complex with the presence of intermediates. The transition midpoint obtained from CD is 4.1 M GdnHCl, where as the midpoints obtained from fluorescence are 1.5 M and 4.0 M GdnHCl (Mohan et al. 2009b). The first transition observed from fluorescence could be either due to the partially collapsed nature of the dimer or due to dimer dissociation. Grimsley *et al.* (1997) suggested that if the first transition of the unfolding is concentration dependent then the intermediate present is a monomeric species and the scheme can be written as $N_2 \Leftrightarrow (2N_I/2N_N) \Leftrightarrow 2U$; where N_2 is the dimer, U is the unfolded and N_I, N_N represent the intermediate monomer and native monomer, respectively. If the second transition of the unfolding is concentration dependent then the intermediate present is a dimeric intermediate and the scheme can be written as $N_2 \Leftrightarrow I_2 \Leftrightarrow 2U$; where I_2 is the dimeric intermediate. The concentration-dependent GdnHCl-induced denaturation studies carried out by Barbar *et al.* (2001) on the DLC8 dimer suggest that the initial unfolding transition is concentration dependent whereas the second unfolding transition is concentration independent. Hence, the unfolding behaviour monitored by fluorescence can be characterized as Dimer ⇔ 2Monomers ⇔ 2Unfolded. The second transition midpoint (~4.1) obtained both from CD and fluorescence can be attributed to unfolding of the monomer. The two-state behaviour of CD data could probably be due to the same secondary structural features of both the dimer and the monomer (Krishna Mohan and Hosur 2007). Further, NMR–HSQC experiment (Mohan *et al.* 2009b) at the first transition midpoint (1.5 M GdnHCl) showed several additional peaks, indicating the presence of at least one other species. Comparison of this spectrum with the HSQC spectrum at 0 M GdnHCl, and also with that of a mutant protein H55K (figure 6B), established that the intermediate species in the first transition was a folded DLC8 monomer. In the former case (0 M GdnHCl), the protein exists as a pure dimer, whereas DLC8–H55K is known to exist as a pure monomer (Nyarko *et al.* 2005).

Further, recently reported native-state hydrogen-exchange (NHX) experiments using NMR spectroscopy have delineated the structural stability and unfolding characteristics of the individual residues in finer detail (Mohan *et al.* 2009a). NHX analysis of the DLC8 dimer has provided valuable insights into the stabilities of the various structural elements of the protein (figure 7A). It is clear from figure 7A that the N-terminal of the protein (aa 1–15), which includes the *β*1-strand, is the least protected. Among the antiparallel *β*-sheets (*β*2, *β*3 and *β*4, *β*5), the *β*3-strand is less stable compared with *β*2 and *β*4, which have almost similar stabilities. However, the *β*5-strand is observed to be the most stable among all the *β*-strands. Further, between the two helices, the stability index suggests that the *α*2-helix
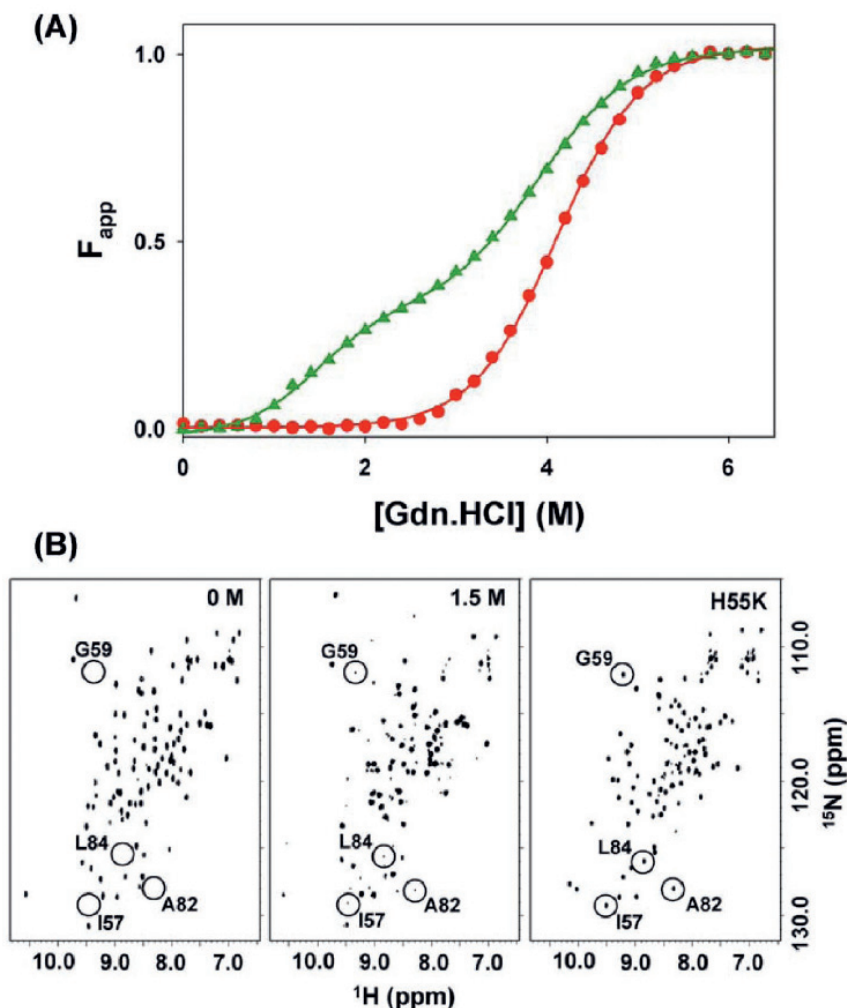
Figure 6. **(A)** Normalized spectroscopic parameters (fraction apparent – F_{app}) obtained from circular dichroism **(circles, red)** and steady-state fluorescence **(triangles, green),** are plotted against concentration of GdnHCl. The solid lines represent the best fits obtained (Mohan *et al.* 2009b). **(B)** $^1H^N$-^{15}N HSQC spectra of DLC8 protein at pH 7, 27°C with GdnHCl concentrations of 0 M (left) and 1.5 M (middle). The spectrum of the H55K mutant, which is a monomer, at pH 7 is shown in the right panel. Residues I57, G59, A82, L84 corresponding to the monomeric species are annotated and marked with circles as illustrative examples.

is more stable than the α1-helix. The higher stability of the α2-helix, β4 and β5 sheets compared with those of the remaining structural elements is consistent with the presence of some residues in there whose peaks did not lose intensity even after 4 months in the NHX experiment (Mohan *et al.* 2009a).

The GdnHCl-dependent NHX experiments provided insights into the nature of unfolding of the individual residues (Mohan *et al.* 2009a). These experiments suggested that the unfolding landscape of the DLC8 dimer is dominated both by global and local fluctuations. The unfolding free energies and the *m-values* obtained for individual residues are shown in figure 7B and 7C to highlight the differences in the unfolding energies and *m-values,* respectively, at different segments of the molecule. Unfolding of the α1-helix has

contributions from both local and global unfolding events, whereas the α2-helix is completely dominated by global unfolding events. A small cooperative unfolding unit has been identified in the α2-helix in the region of A39–Y41; these three residues have almost similar *m-values* and unfolding free energies ($\varDelta G_{uf}$) supporting the fact that their unfolding features are similar (figure 7B and 7C). One more noticeable feature is the increase in unfolding free energy ($\varDelta G_{uf}$) values, i.e. upward slope (*m-value*) with an increase in the GdnHCl concentration for the residues T26 and Q27 in the α1-helix, suggesting a different type of stability in this segment (Brorsson *et al.* 2006; Mohan *et al.* 2009a) (figure 7C right panel). In the case of β-strands, both local and global mechanisms do exist. The residues in the β2−strand are completely dominated by local fluctuations, whereas the
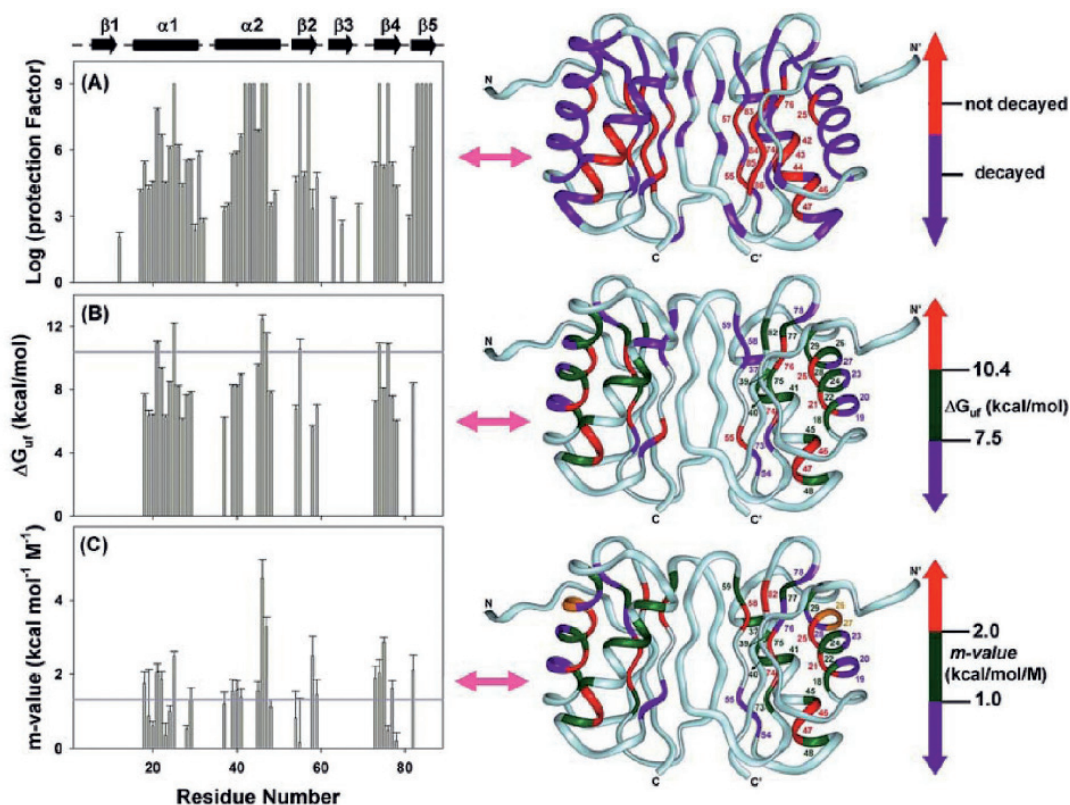
Figure 7. Summary of **(A)** protection factors, **(B)** free energies of unfolding (ΔG_{uf}) and **(C)** *m-value* plotted against the residue number for the individual residues of the DLC8 dimer. The secondary structural elements in the protein are marked above with cylinders (for helices) and arrows (for sheets). The horizontal solid lines in **(B)** and **(C)** represent the global unfolding free energy (ΔG^o) and the *m-value* measured using CD spectroscopy (Mohan *et al.* 2009a), respectively. In **(A),** the right side picture displays the protected residues in a colour-coded manner on the three-dimensional structure of the protein (PDB ID: 1f3c): violet indicates residues that decayed completely within 4 months and red indicates residues that did not exchange at all even after 4 months. Residues that were highly protected are annotated with numbers (red) on one of the monomers for better clarity. Similarly, free energies of unfolding (ΔG_{uf}) and *m-values* shown in **(B)** and **(C)** are marked on the native structure with gradient colouring (violet green red) to show the differences in unfolding energies and degree of solvent accessibility, respectively, at different segments of the molecule. Residues T26 and Q27 whose *m-values* have opposite signatures are shown in yellow colour **(C)**. Residues marked with violet in **(C)** have m-values <1.0 kcal/mol/M and represent local unfolding events. Numbers for all the coloured residues are indicated on one of the monomers only for better clarity. The primed and the unprimed labels distinguish the two monomers. The images were produced using Insight II.

$\beta4$−strand has contributions from global and local unfolding events (figure 7C). Among all the β−strands, $\beta5$ is the most stable as most of the residues (I83 to F86) belonging to this strand remained protected even at a concentration of 0.6 M GdnHCl, indicating that it has considerably high ΔG_{uf} values.

On the basis of all the folding energetics and structural data on the DLC8 protein, a simple model has been proposed by Mohan *et al.* (2009a) to connect the sequential events in the folding process of the DLC8 dimer. The antiparallel β-strands ($\beta4$ and $\beta5$), which form the hydrophobic core of the protein and the $\alpha2$ helix, all of which are highly protected with regard to hydrogen exchange, contribute significantly to the initial step of the protein folding mechanism. This is followed by the formation of the remaining structural elements such as the $\alpha1$-helix and $\beta1$- and $\beta2$-strands. Once the monomer is formed, these two independent monomeric units assemble to associate into a homodimer with the formation of the intervening $\beta3$-strand.

7. Native state ruggedness: near native states and structure adaptability

The shape of the folding funnel around the native state has important implications for a protein's function. A deep well, the bottom of which corresponds to the native state, would imply high stability of the native state. In contrast, a shallow potential well would indicate many low-lying excited states above the native state, and such a situation would be described as a 'rugged native state'. These characteristics

would have significant influence on the dynamics, structural adaptability, or susceptibility of the protein to various functions (Feher and Cavanagh 1999; Piana *et al.* 2002; Parak 2003; Tobi and Bahar 2005; Whitten *et al.* 2005; Kamatari *et al.* 2005; Boehr *et al.* 2006; Mittermaier and Kay 2006 Stockwell and Thornton 2006). This ruggedness or otherwise of the native state ensemble of a given protein can be probed at residue-level detail by NMR by the application of small environmental perturbations such as small concentrations of chemical denaturants, change in pressure, change in pH, etc. (Akasaka 2006; Williamson 2003). In fact, environment-sensitive residues are the ones that play prominent roles in various biological activities such as signal transduction, enzymatic catalysis, macromolecular association, cargo trafficking, etc.

Non-linear temperature dependence or curved temperature dependence of the amide proton chemical shifts provides information about the residues that access alternative states (Baxter *et al.* 1998; Williamson 2003; Tunnicliffe *et al.* 2005; Krishna Mohan *et al.* 2008; Mohan *et al.* 2008). Temperature-dependent studies on the DLC8 dimer in the range 290–315 K by giving a small pH perturbation (pH 7 to pH 6) have provided significant insights into native-state fluctuations (Krishna Mohan *et al.* 2008). Residues accessing alternative states at pH 7 (figure 8) furnish the details of the segments that contribute to native-state ruggedness, whereas residues that access curvature at only pH 6 indicate the sensitivity of conformational dynamics to environmental perturbations. The results at both the pH

values (7 and 6) put together indicate the overall adjustability in the native state, since neither of the pH perturbations takes the protein out of the native-state ensemble. The number of residues accessing alternative conformations in the dimer at pH 7 and 6 are 13 and 21, respectively (figure 9A). The locations of these residues are marked in red colour on the native structure of the dimeric protein in figures 9B and 9C. Overall, the number for residues that can access alternative conformations considering either of the pH values are: 25 for the dimer (figure 9A), which is >25% of the total number of residues in the protein.

It is evident from figure 9 that the C-terminal *β*-sheets are more dynamic in the dimer compared with the N-terminal helices. The perturbations observed at these sites have functional significance, as small pH differences are known to exist in different parts of a cell (Stewart *et al.* 1999; Vaughan-Jones *et al.* 2002; Willoughby and Schwiening 2002; Spitzer and Poolman 2005; Swietach *et al.* 2005), and several of the residues that access low-energy excited states surround the dimer interface of the molecule, which is also the cargo-binding site (Liang *et al.* 1999). It can be envisaged that the observed sensitivity of conformational dynamics at the dimer interface due to small environmental perturbations can significantly influence the cargo-binding nature of the protein. Theoretical simulations have provided information on the range of free energies of the near-native states accessed by the fluctuating residues and indicate that the alternative states lie within 2–3 kcal/mol from the ground state (Krishna Mohan *et al.* 2008).
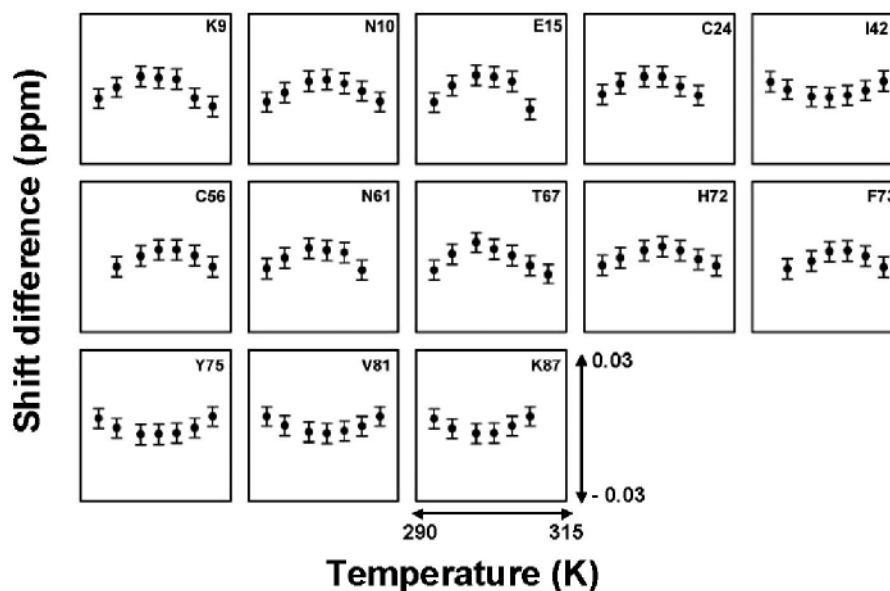

Figure 8. Residues showing non-linear temperature dependence of amide proton chemical shifts in DLC8 measured at pH 7.0. The measured chemical shifts were fitted to a linear equation. The residuals (observed value – calculated value according to the linear fit) have been plotted against temperature; total scale of the Y-axis is 0.06 ppm: +0.03 to –0.03 centred at zero, and the temperature range is 290 K–315 K. The error bars give an indication of the approximate error in measured chemical shifts (±0.004 ppm).
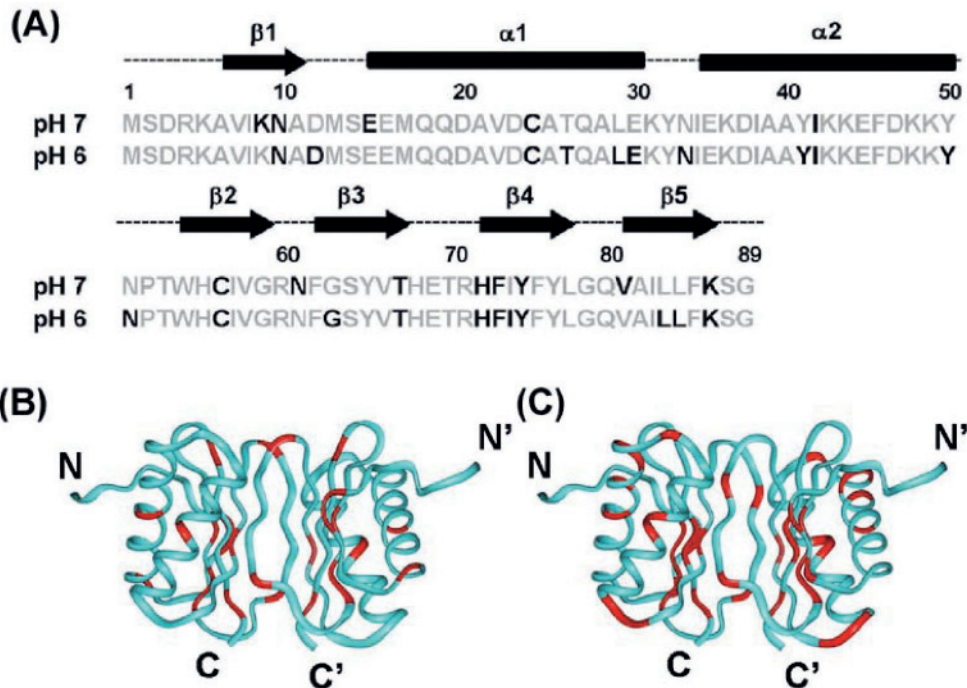
Figure 9. **(A)** Residues showing non-linear temperature dependence of amide proton chemical shifts (black) along the polypeptide chain. *The results* are shown for pH 7.0 and 6.0. The arrows (β−strands) and cylinders (α−helices) indicate native secondary structures. Residues exhibiting curved temperature dependence in DLC8 dimer **(B)** pH 7.0, **(C)** pH 6.0 (PDB Id: 1f3c) are coloured red on the three-dimensional structure of the protein. The image was produced using Insight II.

The roughness of the energy landscape and the consequent fluctuations in the native state of a protein is a reflection on the nature of the interactions between the side chains of different amino acid residues in the three-dimensional structure of the protein. Although this is not generally predictable, insights may be obtained in some cases by closely examining the structure and properties of the amino acids (titratable groups, electrostatic potentials, etc.) along the sequence. In the case of the dimer, the sensitivity of conformational dynamics can be readily traced to partial protonation of the His side chains as discussed in the previous section. There will be interconversions between charged and neutral His (His 68 and His 72) and there will also be charge–charge repulsions. These will cause fluctuations in local electrostatic potentials, and consequently in local side chain packing which, in turn, will affect conformations in the main chain.

8. Modulation of target-binding efficacy

As mentioned in the previous sections, structural studies have revealed that the dimer binds its target molecules in an anti-parallel β-strand fashion through its β3-strand, and also forms several contacts with the residues that are present at the dimer interface. Moreover, dynamics and mutational investigations on the DLC8 dimer (Nyarko *et al.* 2005; Mohan *et al.* 2006; Krishna Mohan and Hosur 2007; Song

et al. 2007, 2008; Krishna Mohan *et al.* 2008; Mohan and Hosur 2008b; Mohan *et al.* 2009b) have pointed out that the dimeric molecule is highly dynamic and the alteration of such dynamics due to small environmental perturbations can regulate the target-binding efficacy as these dynamic residues are mainly clustered around the dimer interface/ cargo-binding region. In this context, cargo-binding studies on the DLC8 dimer under a small environmental perturbation (pH values 7 and 6) by saturation with an 11 residue fragment of IC74 (dynein intermediate chain) containing the binding motif (K/R)XTQT as a cargo representative, have elucidated the regulatory role of protein dynamics in modulating target-binding efficacies (Krishna Mohan and Hosur 2007; Mohan and Hosur 2008b). Figure 10A shows the spectrum of free DLC8 at pH 7. The HSQC spectrum at pH 7 in the presence of the peptide (figure 10B) has nearly the same number of peaks as the spectrum in the absence of the peptide (figure 10A), though some peaks have shifted positions due to peptide interaction. The HSQC spectrum at pH 6 in the presence of the peptide (figure 10C) has several more peaks, which indicates coexistence of multiple species. Many of the peaks can be identified with the free dimer, indicating that the ensemble consists of both bound and free dimers. For example, peaks due to D37, I38, which had moved to positions indicated by circles on peptide binding at pH 7, acquire some intensity at their

positions in the free dimer (indicated by squares) at pH 6, suggesting partial dissociation of the complex. This clearly indicates that the efficacy of binding has reduced compared

to that at pH 7 (figure 10C). However, the major population at pH 6 is still the bound species as is evident from the low intensities of the peaks belonging to the free protein. These studies demonstrate that the efficacy of DLC8 dimer binding to the peptide is sensitive to pH.
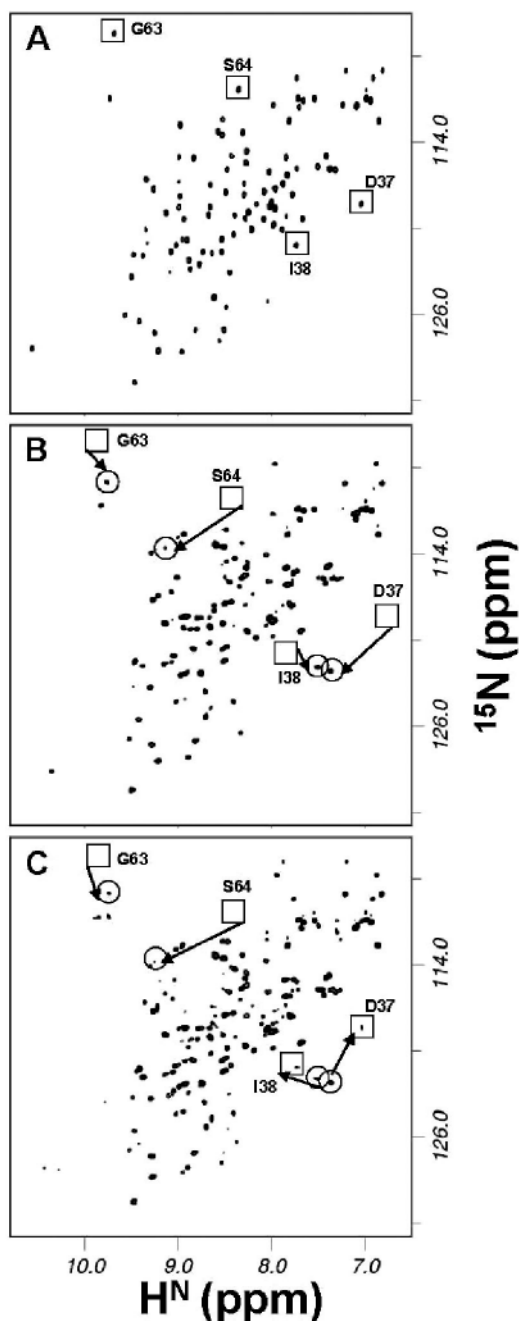
9.   Regulatory functional implications

The DLC8 dimer transports different cellular machinery across the cell. During cargo trafficking, it has to encompass small folding/unfolding events and encounter structural/ dynamic fluctuations in order to facilitate loading/unloading of cargo molecules. The GdnHCl/pH-induced dissociation/ unfolding of the DLC8 dimer has furnished rationales for the structural and dynamic aspects of the protein, which is crucial for its cargo adaptability and trafficking. It is evident that the β3-strand and the intervening β3–β4 loop are highly solvent accessible (figure 7A). Moreover, it is interesting to note that the residues in the β2-strand, which forms an antiparallel sheet with the β3-strand of the monomer, and the β4-strand, which forms important contacts with the target along with the β3-strand, are highly dominated by local fluctuations (figure 7C). Considering that the DLC8 dimer should be adaptable for targeting several proteins of different topologies, the structural features of the free and peptide bound dimer are similar (Liang *et al.* 1999; Fan *et al.* 2001) and, in light of the folding features reported, it is evident that the dimer molecule loads/ unloads its targets through minor adjustments such as local fluctuation/unfolding within the immediate neighbouring structural elements comprising β2 and β4 sheets. Further, as monomeric DLC8 protein is not capable of binding any of the target molecules (Wang *et al.* 2003), it is suggested that the topology and stability of the dimer dictate cargo loading/unloading. Small environmental perturbations can efficiently modulate target-binding efficacies by regulating the dynamics of the dimer. It is well known that the cytoplasm consists of pools of heterogeneous compartments with small pH/electrolyte differences. This heterogeneity is a result of localized acid–base catalysed enzymatic reactions and low mobility of the ions (Spitzer and Poolman 2005). In this background, it is extremely interesting to note that the dimer interface of DLC8, which is also the cargo-binding site, exhibits significant conformational dynamics, and is sensitive to environmental conditions (pH, GdnHCl, etc.). Similar local unfolding events in response to other environmental perturbations such as ionic strength changes, metabolite concentration changes, some small molecule interactions, etc. can also be anticipated. These observed dynamics would account for the adaptability of the DLC8 dimer as per the demand of various target molecules and facilitate the cargo binding and release required for trafficking inside the cell.

Figure 10. ^{1}H – ^{15}N HSQC spectra of DLC8. **(A)** Free DLC8 at pH 7. **(B, C)** DLC8 in the presence of peptide at pH 7 **(B)** and at pH 6 **(C)**. Peak shifts for a few residues, D37, I38, G63 and S64 have been shown for illustration. Squares identify the peaks in the free protein and circles identify the peaks in the protein–peptide complex. Arrow directions indicate the flow of the intensity as the pH is reduced.

Acknowledgements

References

Akasaka K 2006 Probing conformational fluctuation of proteins by pressure perturbation; *Chem Rev.* **106** 1814–1835

Barbar E 2008 Dynein light chain LC8 is a dimerization hub essential in diverse protein networks; *Biochemistry* **47** 503–508

Barbar E and Hare M 2004 Characterization of the cargo attachment complex of cytoplasmic dynein using NMR and mass spectrometry; *Methods Enzymol.* **380** 219–241

Barbar E, Kleinman B, Imhoff D, Li M, Hays T S and Hare M 2001 Dimerization and folding of LC8, a highly conserved light chain of cytoplasmic dynein; *Biochemistry* **40** 1596–1605

Baxter N J, Hosszu L L, Waltho J P and Williamson M P 1998 Characterisation of low free-energy excited states of folded proteins; *J. Mol. Biol.* **284** 1625–1639

Benashski S E, Harrison A, Patel-King R S and King S M 1997 Dimerization of the highly conserved light chain shared by dynein and myosin V; *J. Biol. Chem* **272** 20929–20935

Boehr D D, McElheny D, Dyson H J and Wright P E 2006 The dynamic energy landscape of dihydrofolate reductase catalysis; *Science* **313** 1638-1642.

Brorsson A C, Lundqvist M, Sethson I and Jonsson B H 2006 GuHCl and NaCl-dependent hydrogen exchange in MerP reveals a well-defined core with an unusual exchange pattern; *J. Mol. Biol.* **357** 1634–1646

Bryngelson J D, Onuchic J N, Socci N D and Wolynes P G 1995 Funnels, pathways, and the energy landscape of protein folding: a synthesis; *Proteins* **21** 167–195

Chatterjee A, Krishna Mohan P M, Prabhu A, Ghosh-Roy A and Hosur R V 2007 Equilibrium unfolding of DLC8 monomer by urea and guanidine hydrochloride: distinctive global and residue level features; *Biochimie* **89** 117–134

Crepieux P, Kwon H, Leclerc N, Spencer W, Richard S, Lin R and Hiscott J 1997 I kappaB alpha physically interacts with a cytoskeleton-associated protein through its signal response domain; *Mol. Cell Biol.* **17** 7375–7385

Dick T, Ray K, Salz H K and Chia W 1996 Cytoplasmic dynein (ddlc1) mutations cause morphogenetic defects and apoptotic cell death in *Drosophila melanogaster*; *Mol. Cell Biol.* **16** 1966–1977

Dill K A and Chan H S 1997 From Levinthal to pathways to funnels; *Nat. Struct. Biol.* **4** 10–19

Dobson C M 2003 Protein folding and misfolding; *Nature* (London) **426** 884–890

Dobson C M and Karplus M 1999 The fundamentals of protein folding: bringing together theory and experiment; *Curr. Opin. Struct. Biol.* **9** 92–101

Dunker A K, Brown C J, Lawson J D, Iakoucheva L M and Obradovic Z 2002 Intrinsic disorder and protein function; *Biochemistry* **41** 6573–6582

Dyson H J and Wright P E 2005 Elucidation of the protein folding landscape by NMR; *Methods Enzymol.* **394** 299–321

Fan J, Zhang Q, Tochio H, Li M and Zhang M 2001 Structural basis of diverse sequence-dependent target recognition by the 8 kDa dynein light chain; *J. Mol. Biol.* **306** 97–108

Fan J S, Zhang Q, Tochio H and Zhang M 2002 Backbone dynamics of the 8 kDa dynein light chain dimer reveals molecular basis of the protein's functional diversity; *J. Biomol. NMR* **23** 103–114

Feher V A and Cavanagh J 1999 Millisecond-timescale motions contribute to the function of the bacterial response regulator protein Spo0F; *Nature (London)* **400** 289–293

Grimsley J K, Scholtz J M, Pace C N and Wild J R 1997 Organophosphorus hydrolase is a remarkably stable enzyme that unfolds through a homodimeric intermediate; *Biochemistry* **36** 14366–14374

Harrison A and King S M 2000 The molecular anatomy of dynein; *Essays Biochem.* **35** 75–87

Herzig R P, Andersson U and Scarpulla R C 2000 Dynein light chain interacts with NRF-1 and EWG, structurally and functionally related transcription factors from humans and drosophila; *J. Cell Sci.* **113 Pt 23** 4263–4273

Hook P and Vallee R B 2006 The dynein family at a glance; *J. Cell Sci.* **119** 4369–4371

Jaffrey S R and Snyder S H 1996 PIN: an associated protein inhibitor of neuronal nitric oxide synthase; *Science* **274** 774–777

Kamatari Y O, Yokoyama S, Tachibana H and Akasaka K 2005 Pressure-jump NMR study of dissociation and association of amyloid protofibrils; *J. Mol. Biol.* **349** 916–921

King S M 2000 The dynein microtubule motor; *Biochim. Biophys. Acta* **1496** 60–75

King S M, Barbarese E, Dillman J F, III, Patel-King R S, Carson J H and Pfister K K 1996a Brain cytoplasmic and flagellar outer arm dyneins share a highly conserved Mr 8,000 light chain; *J. Biol. Chem.* **271** 19358–19366

King S M, Dillman J F, III, Benashski S E, Lye R J, Patel-King R S and Pfister K K 1996b The mouse t-complex-encoded protein Tctex-1 is a light chain of brain cytoplasmic dynein; *J. Biol. Chem.* **271** 32281–32287

King S M and Patel-King R S 1995 The M(r) = 8,000 and 11,000 outer arm dynein light chains from Chlamydomonas flagella have cytoplasmic homologues; *J. Biol. Chem.* **270** 11445–11452

Koradi R, Billeter M and Wuthrich K 1996 MOLMOL: a program for display and analysis of macromolecular structures; *J. Mol. Graph.* **14** 51–32

Krishna Mohan P M 2007 Unfolding energetics and conformational stability of DLC8 monomer; *Biochimie* **89** 1409–1415

Krishna Mohan P M, Barve M, Chatterjee A, Ghosh-Roy A and Hosur R V 2008 NMR comparison of the native energy landscapes of DLC8 dimer and monomer; *Biophys. Chem.* **134** 10–19

Krishna Mohan P M, Chakraborty S and Hosur R V 2009 NMR investigations on residue level unfolding thermodynamics in DLC8 dimer by temperature dependent native state hydrogen exchange; *J. Biomol. NMR* **44** 1–11

Krishna Mohan P M and Hosur R V 2007 NMR insights into dynamics regulated target binding of DLC8 dimer; *Biochem. Biophys. Res. Commun.* **355** 950–955

Leopold P L, Kreitzer G, Miyazawa N, Rempel S, Pfister K K, Rodriguez-Boulan E and Crystal R G 2000 Dynein- and microtubule-mediated translocation of adenovirus serotype 5 occurs after endosomal lysis; *Hum. Gene Ther.* **11** 151–165

Levinthal C 1969 *Mössbauer spectroscopy in biological systems* (eds) J T P DeBrunner and E Munck (Illinois: University of Illinois Press) pp 22–24

Liang J, Jaffrey S R, Guo W, Snyder S H and Clardy J 1999 Structure of the PIN/LC8 dimer with a bound peptide; *Nat. Struct. Biol.* **6** 735–740

Lo K W, Naisbitt S, Fan J S, Sheng M and Zhang M 2001 The 8-kDa dynein light chain binds to its targets via a conserved (K/R)XTQT motif; *J. Biol. Chem.* **276** 14059–14066

Makokha M, Huang Y J, Montelione G, Edison A S and Barbar E 2004 The solution structure of the pH-induced monomer of dynein light-chain LC8 from *Drosophila*; *Protein Sci.* **13** 727–734

Mittermaier A and Kay L E 2006 New tools provide new insights in NMR studies of protein dynamics; *Science* **312** 224–228

Mohan P M, Barve M, Chatterjee A and Hosur R V 2006 pH driven conformational dynamics and dimer-to-monomer transition in DLC8; *Protein Sci.* **15** 335–342

Mohan P M, Chakraborty S and Hosur R V 2009a Residue-wise conformational stability of DLC8 dimer from native-state hydrogen exchange; *Proteins* **75** 40–52

Mohan P M and Hosur R V 2008b NMR characterization of structural and dynamics perturbations due to a single point mutation in *Drosophila* DLC8 dimer: functional implications; *Biochemistry* **47** 6251–6259

Mohan P M and Hosur R V 2008a pH dependent unfolding characteristics of DLC8 dimer: residue level details from NMR; *Biochim. Biophys. Acta* **1784** 1795–1803

Mohan P M, Joshi M V and Hosur R V 2009b Hierarchy in guanidine unfolding of DLC8 dimer: regulatory functional implications; *Biochimie* **91** 401–407

Mohan P M, Mukherjee S and Chary K V 2008 Differential native state ruggedness of the two Ca2+-binding domains in a Ca2+ sensor protein; *Proteins* **70** 1147–1153

Naisbitt S, Valtschanoff J, Allison D W, Sala C, Kim E, Craig A M, Weinberg R J and Sheng M 2000 Interaction of the postsynaptic density-95/guanylate kinase domain-associated protein complex with a light chain of myosin-V and dynein; *J. Neurosci.* **20** 4524–4534

Navarro-Lerida I, Martinez M M, Roncal F, Gavilanes F, Albar J P and Rodriguez-Crespo I 2004 Proteomic identification of brain proteins that interact with dynein light chain LC8; *Proteomics* **4** 339–346

Nyarko A, Cochrun L, Norwood S, Pursifull N, Voth A and Barbar E 2005 Ionization of His 55 at the dimer interface of dynein light-chain LC8 is coupled to dimer dissociation; *Biochemistry* **44** 14248–14255

Onuchic J N, Luthey-Schulten Z and Wolynes P G 1997 Theory of protein folding: the energy landscape perspective; *Annu. Rev. Phys. Chem.* **48** 545–600

Parak F G 2003 Proteins in action: the physics of structural fluctuations and conformational changes; *Curr. Opin. Struct. Biol.* **13** 552–557

Pfister K K 2005 Dynein cargo gets its groove back; *Structure (Camb.)* **13** 172–173

Pfister K K, Salata M W, Dillman J F, III, Torre E and Lye R J 1996 Identification and developmental regulation of a neuron-specific subunit of cytoplasmic dynein; *Mol. Biol. Cell* **7** 331–343

Piana S, Carloni P and Parrinello M 2002 Role of conformational fluctuations in the enzymatic reaction of HIV-1 protease; *J. Mol. Biol.* **319** 567–583

Puthalakath H, Huang D C, O'Reilly L A, King S M and Strasser A 1999 The proapoptotic activity of the Bcl-2 family member Bim is regulated by interaction with the dynein motor complex; *Mol. Cell* **3** 287–296

Puthalakath H, Villunger A, O'Reilly L A, Beaumont J G, Coultas L, Cheney R E, Huang D C and Strasser A 2001 Bmf: a proapoptotic BH3-only protein regulated by interaction with the myosin V actin motor complex, activated by anoikis; *Science* **293** 1829–1832

Rodriguez-Crespo I, Yelamos B, Roncal F, Albar J P, Ortiz de Montellano P R and Gavilanes F 2001 Identification of novel cellular proteins that bind to the LC8 dynein light chain using a pepscan technique; *FEBS Lett.* **503** 135–141

Schnorrer F, Bohmann K and Nusslein-Volhard C 2000 The molecular motor dynein is involved in targeting swallow and bicoid RNA to the anterior pole of *Drosophila* oocytes; *Nat. Cell Biol.* **2** 185–190

Shoemaker B A, Wang J and Wolynes P G 1999 Exploring structures in protein folding funnels with free energy functionals: the transition state ensemble; *J. Mol. Biol.* **287** 675–694

Sodeik B, Ebersold M W and Helenius A 1997 Microtubule-mediated transport of incoming herpes simplex virus 1 capsids to the nucleus; *J. Cell Biol.* **136** 1007–1021

Song C, Wen W, Rayala S K, Chen M, Ma J, Zhang M and Kumar R 2008 Serine 88 phosphorylation of the 8-kDa dynein light chain 1 is a molecular switch for its dimerization status and functions; *J. Biol. Chem* **283** 4004–4013

Song Y, Benison G, Nyarko A, Hays T S and Barbar E 2007 Potential role for phosphorylation in differential regulation of the assembly of dynein light chains; *J. Biol. Chem.* **282** 17272–17279

Spitzer J J and Poolman B 2005 Electrochemical structure of the crowded cytoplasm; *Trends Biochem. Sci.* **30** 536–541

Stewart A K, Boyd C A and Vaughan-Jones R D 1999 A novel role for carbonic anhydrase: cytoplasmic pH gradient dissipation in mouse small intestinal enterocytes; *J. Physiol.* **516 (Pt 1)** 209–217

Stockwell G R and Thornton J M 2006 Conformational diversity of ligands bound to proteins; *J. Mol. Biol.* **356** 928–944

Suomalainen M, Nakano M Y, Keller S, Boucke K, Stidwill R P and Greber U F 1999 Microtubule-dependent plus- and minus end-directed motilities are competing processes for nuclear targeting of adenovirus; *J. Cell Biol.* **144** 657–672

Swietach P, Leem C H, Spitzer K W and Vaughan-Jones R D 2005 Experimental generation and computational modeling of

intracellular pH gradients in cardiac myocytes; *Biophys. J.* **88** 3018–3037

Tobi D and Bahar I 2005 Structural changes involved in protein binding correlate with intrinsic motions of proteins in the unbound state; *Proc. Natl. Acad. Sci. USA* **102** 18908–18913

Tochio H, Ohki S, Zhang Q, Li M and Zhang M 1998 Solution structure of a protein inhibitor of neuronal nitric oxide synthase; *Nat. Struct. Biol.* **5** 965–969

Tunnicliffe R B, Waby J L, Williams R J and Williamson M P 2005 An experimental investigation of conformational fluctuations in proteins G and L; *Structure (Camb.)* **13** 1677–1684

Uversky V N 2002 Natively unfolded proteins: a point where biology waits for physics; *Protein Sci.* **11** 739–756

Vadlamudi R K, Bagheri-Yarmand R, Yang Z, Balasenthil S, Nguyen D, Sahin A A, Den H P and Kumar R 2004 Dynein light chain 1, a p21-activated kinase 1-interacting substrate, promotes cancerous phenotypes; *Cancer Cell* **5** 575–585

Vallee R B, Williams J C, Varma D and Barnhart L E 2004 Dynein: an ancient motor protein involved in multiple modes of transport; *J. Neurobiol.* **58** 189–200

Vaughan-Jones R D, Peercy B E, Keener J P and Spitzer K W 2002 Intrinsic H(+) ion mobility in the rabbit ventricular myocyte; *J. Physiol.* **541** 139–158

Wang W, Lo K W, Kan H M, Fan J S and Zhang M 2003 Structure of the monomeric 8-kDa dynein light chain and mechanism of the domain-swapped dimer assembly; *J. Biol. Chem.* **278** 41491–41499

Whitten S T, Garcia-Moreno E B and Hilser V J 2005 Local conformational fluctuations can modulate the coupling between proton binding and global structural transitions in proteins; *Proc. Natl. Acad. Sci. USA* **102** 4282–4287

Williamson M P 2003 Many residues in cytochrome c populate alternative states under equilibrium conditions; *Proteins* **53** 731–739

Willoughby D and Schwiening C J 2002 Electrically evoked dendritic pH transients in rat cerebellar Purkinje cells; *J. Physiol.* **544** 487–499

Wolynes P G 2005 Energy landscapes and solved protein-folding problems; *Philos. Transact. A Math. Phys. Eng. Sci.* **363** 453–464

Wolynes P G, Onuchic J N and Thirumalai D 1995 Navigating the folding routes; *Science* **267** 1619–1620

Yang Z, Vadlamudi R K and Kumar R 2005 Dynein light chain 1 phosphorylation controls macropinocytosis; *J. Biol. Chem.* **280** 654–659